Proving Actinide Contraction in Solution

DOI: 10.1002/anie.200((will be filled in by the editorial staff))

Solving the hydration structure of the heaviest actinoid aquaion known: the Californium(III) case

Elsa Galbis Fuster, Jorge Hernández-Cobos, Christophe den Auwer, Claire Le Naour, Dominique Guillaumont, Eric Simoni, Rafael R. Pappalardo and Enrique Sánchez Marcos**

The solution chemistry of actinoid ions has been a fundamental question since the beginning of the nuclear technologies. The stability of high oxidation states of actinides in solution is intimately linked to the nuclear technology.[1] The investigation of procedures which avoid the migration of actinides in natural water systems in the framework of the already accumulated nuclear waste disposal in geological formations is a field of great activity.[2] One of the primary research needs of actinoid ions in solution is the characterization of its closest solvation structure, since it is at the heart of the further complexation, precipitation and resolution processes. The rareness and hazardousness of the heavier actinide elements, which steeply increase with the atomic number, has prevented a complete examination of the trends along the series, beyond the middle of the series.[3] Curium cation, Cm(III) has often been considered as the heaviest actinide species characterized, having attracted much attention from both experimental and theoretical views in recent years.[3,4] Systematic studies of the aqueous trivalent lanthanoids have long been pointed out that a contraction of the metal-oxygen distance and a decreasing of the total first coordination number along the series is observed.[5] Recent works have examined using EXAFS technique if this contraction takes place in a monotone or an irregular way along the series.[6] The data available for the actinide series up to Cm(III) indicates a similar trend,[3,7] although a conclusive answer can not be given, since the uncertainty of the structural data and the scarce information on the second half of the series. Beyond the middle of the series, there is only one study reported for berkelium, Bk(III)[8] and a preliminary EXAFS study for Cf(III) carried out by one of us.[9] Due to the position of Cf(III) an accurate enough determination of the coordination number and Cf-O distance could certainly shed light on the question of the actinide contraction, taking this objective a character more fundamental than applied since the extremely rareness of this element. However, the absence of available crystallographic data of Cf(III) with appropriate Cf-O bonds to be used as structural reference precludes the required level of accuracy for answering the question on the basis of a conventional EXAFS data analysis.

This letter presents an alternative way of study for this extreme case, by coupling new highly refined EXAFS data obtained in an actinide dedicated beamline in the third generation European Synchrotron Radiation Facility (ESRF, Grenoble), with the first Monte Carlo simulations of Cf(III) in water. Specifically developed Cf-H_2O intermolecular potentials based on ab initio quantum mechanical (QM) potentials energy surfaces and the polarisable and flexible MCDHO water model [10] have been used.

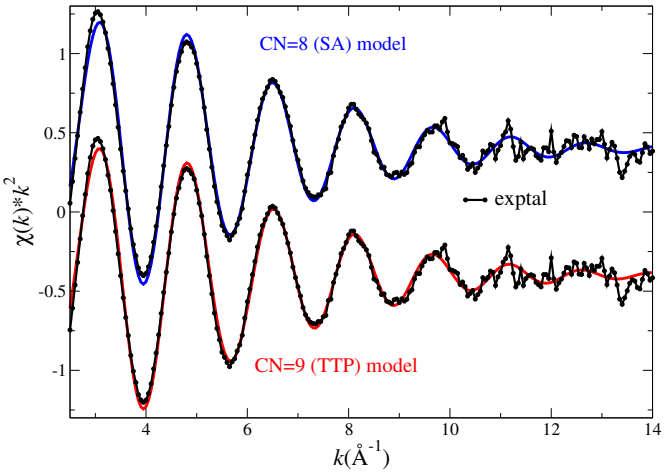

Figure 1. Experimental (black line) and fitted (red and blue lines) Cf L_{III}-edge EXAFS spectrum of Cf(III) aqueous solution, using as aquaion model the Square Antiprism (CN=8) (top) and the Trigonal tricapped prism (CN=9) (bottom).

Figure 1 shows the experimental and fitted k^2-weighted EXAFS spectra of a Cf(III) aqueous solution using two model structures, the square antiprism configuration (SA) (see Fig. 2a) which represents an octa-coordination of water molecules, and the trigonal tricapped prism (TTP) (see Fig. 2c) which implies an ennea-coordination. Since no experimental estimation of the global amplitude factor S_o^2 can be obtained for the Californium case, during the fitting procedure the coordination numbers were fixed to the model values of 8 and 9, respectively. Best fit EXAFS parameters derived from both fits are collected in Table 1. There is no clear visible difference between the two fitted curves and none of the adjusted parameters of Table 1 may allow the rejection of one of the two structural models. Furthermore, the weighted averages of the Cf-O distances are comparable: 8 oxygen atoms at 2.42 Å for SA, 9 oxygen atoms at 2.41 Å for TTP, keeping in mind that a difference of one unit in

[*] Ms. E.Galbis, Dr. R.R.Pappalardo, Prof. E.Sánchez Marcos
Departamento de Química Física.
Universidad de Sevilla
41012-Sevilla (Spain)
Fax: (+34) 954557174
E-mail: sanchez@us.es
Dr. J. Hernández-Cobos
Instituto de Ciencias Físicas,
Apartado Postal 48-3
62251 Cuernavaca (México)
Dr. C. den Auwer, Dr. D. Guillaumont,
CEA,Nuclear Energy Division,
Radiochemistry Process Department , SCPS/LILA
F-30207 Bagnols sur Cèze (France)
E-mail:christophe.denauwer@cea.fr
Dr. C. Le Naour , Prof. E. Simoni
Institut de Physique Nucleaire Orsay,
Univ. Paris-Sud (France)

[ ] Junta de Andalucia (Project number P06-FQM-01484) is acknowleged for financial support. ESRFand FZDR are acknowledged for beamtime allocation at the BM20/ROBL beamline. We are indebted for the loan of ^{249}Cf through the US Department of Energy via the High Flux Isotope Reactor and Radioelement Development Centre of Oak Ridge NL.

coordination number over 9 (11%) is not significant from the EXAFS point of view and especially in the absence of experimental S_0^2 value. The value fitted is 0.9 which is equal to the value obtained for a Pu(III) aqueous solution EXAFS spectrum recorded at the same beamline,[11] and similar to the S_0^2 value of 1 employed by Soderhlom et al. when studying the Cm(III) case.[3a] The model of an uniform ennea-coordination leads to fitting results quite close to those obtained for the SA model, showing a similar Cf-O distance, but with its associated DW factor slightly higher and the S_o^2 value slightly smaller than for the octahydrate model. The Debye-Waller factor (σ^2) for the SA model is relatively higher (0.0077 Å^2) than those of the TTP configuration for their two sets of Cf-O distances in the ennea-hydrate. This could suggest a significant distortion of the hydration shell in the SA configuration. Indeed, Debye-Waller factors for both TTP shells are significantly lower (0.0039 and 0.0068 Å^2). These results also indicate that the 3 capping oxygens are less disordered than the 6 prismatic ones. Skanthakumar *et al.,* for the Cm(III) case, give a small value for the SA model (0.0071 Å^2),[3] whereas the relative values for the DW factors corresponding to the two different Cm-O distances were exchanged with respect to the Cf(III) case when the TTP model was employed.[3] In two recent related papers on the crystal and aqueous structures of lanthanoid(III) aquaions,[6] the Sm(III) case shows similar DW factor distributions to the Cf(III) one, whereas others cations such as La(III) and Dy(III) are more similar to the Cm(III) case. In the present study, attempts to force the same relative values for the Debye-Waller factors in the TTP model have failed and all lead to significantly degraded fits. Contrary to what is observed for Cm(III) and Ln(III) in aqueous solution, distinction between a TTP and an SA configuration can not be unambiguously deduced from the fittings performed in this work.

Table 1. Best fit parameters (Cf-O distance, Debye-Waller factors and $\mathcal{R}$ factor of the fit) for the Cf L_{III}-edge EXAFS spectrum, using as aquaion model either the Square Antiprism (SA) polyhedron or the Trigonal Tricapped Prism (TTP).

Model	$R_{Cf\text{-}O}$ (Å)	σ^2 (Å^2)	$\mathcal{R}$
SA (CN=8)[a]	2.42(1)	0.0077	1.9
TTP (CN=9)[b]	2.38(1)x6	0.0068	1.9
	2.47(1)x3	0.0039	

[a] S_o^2= 0.9, E_o= 1.76 eV, ε=0.0033, $\Delta\chi^2_v$ =0.2
[b] S_o^2= 0.9, E_o= 1.76 eV, ε=0.0033, $\Delta\chi^2_v$ =0.2

Computer simulation of Cf(III) in water represents a completely independent approach to the study of this system. However, no intermolecular Cf(III)-H_2O potential has been proposed in the literature to carry out classical Monte Carlo(MC) or Molecular Dynamics (MD) simulations. Nor have ab initio MD simulations been carried out. In this work, we have developed two independent sets of Cf-H_2O intermolecular potentials based on ab initio potential energy surfaces. We have taken advantage of the QM methodology developed by Dolg and col.[12a] for the trivalent actinoids. They used the MP2 level and DFT by applying the BP86 functional in the QM study of the $[An(H_2O)_n]^{3+}$ series for n=7,8 and 9. A set of quasi-relativistic An(III) 5f-core pseudopotentials were specifically developed to this objective.[12b] These authors included the solvent effects on the possible aquaions by means of the PCM continuum model. They conclude that the hydration number must be ranged between 8 and 9 water molecules for the An(III). We use these two different QM models since according to Dolg et al.'s study [12a] the BP86 method leads to favour the octacoordination, whereas the MP2 method favours higher coordination, close to 9. In this way, the two computer simulations derived from them may then represent a reasonable range of the Cf(III) hydration number.

The model of Cf-water intermolecular potential has been inspired in the hydrated ion concept which has proven its good performance in the computer simulations of other highly-charged metal cations.[13] In its original formulation, the model assumes a high stability of the hydrated ion, such that the exchange of water molecules between the first and the second hydration shell is prevented. Whereas this is a consistent assumption for cations such as Cr(III), Rh(III), Ir(III) or Mg(II), this is not longer valid for large cations such as actinoids or lanthanoids. Thus, to improve our original hydrated ion model, a polarisable and flexible water model, the MCDHO model[13] has been adopted, and the Cf(III) ion has also been described as a polarisable particle. Two intermolecular Cf(III)-H_2O potential was extracted from the potential energy surfaces formed by one cation and a variable set of water molecules, $[Cf(H_2O)_n\cdot(H_2O)]^{3+}$ (between 7 and 9), by scanning the release of a water molecule from the closest environment of the cation in the presence of the rest of first-shell water molecule at the BP86 and MP2 levels. Figure 2 shows the BP86 optimized structures for the octa- and ennea-hydrate (a and c) as well as structures corresponding to the scans releasing a water molecule from the octahydrate (b) or the ennea-hydrate (d).

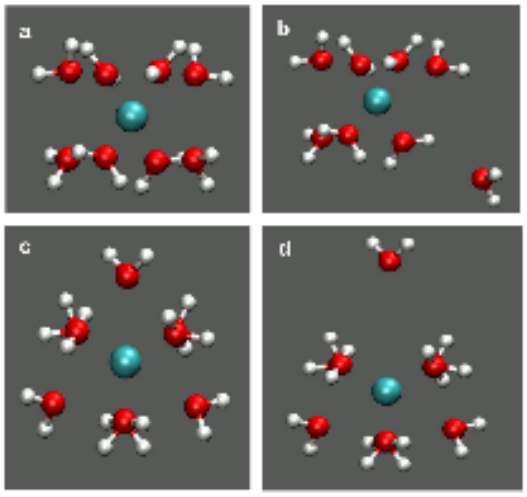

Figure 2. Some structures used for the construction of the Cf(III)-H2O intermolecular potential: (a) and (c) are the BP86 optimized geometries for the octahydrate and enneahydrate. (b) and (d) are distorted structures where one of the water molecules is realeased from its equilibrium position.

The QM global formation energy, ΔE_{form}, of the $[Cf(H_2O)_n]^{3+}$ cluster is decomposed into the different contributions of the molecules involved in the cluster and fitted to a pair-potential, U_{inter}:

$$\Delta E_{form} = E_{[Cf(H_2O)_n]^{3+}} - E_{Cf^{3+}} - nE_{H_2O} = U_{inter} = \sum_{i=1}^{N}\sum_{j>i}^{N} U_{ij}(r_{ij})$$

where the polarisable character of the californium and the water molecule, in addition to the flexible character of the water molecule, allow an individual nuclear and charge distribution relaxation of every molecule of the cluster; although the fitted coefficients of the $U_{ij}(r_{ij})$ are common. This method of building the intermolecular potential collects to a large extent the many-body interactions up to roughly the 9-th order, particularly in the first hydration shell where these interactions are more important.[13] The flexible and polarisable character of the water model allows a proper tuning of the strong polarization changes suffered by the water molecule when going from the first- to outer hydration shells. Further details about

the development and performance of the new potential can be found elsewhere.[14] These two potentials have been tested by comparing the results predicted by the intermolecular potentials with the QM results of the octahydrate and ennea-hydrate aquaions, as well as their hydrated forms, $[Cf(H_2O)_8]^{3+}\cdot(H_2O)_{16}$ and $[Cf(H_2O)_9]^{3+}\cdot(H_2O)_{18}$. In the supporting information the ΔE_{form} values (Table S1) and the optimized structures (Figure S1) are compared. Both sets of results support the good behaviour of the potentials and their energy gradients.

MC simulations for a system formed by 1 Cf(III) + 500 H_2O at 300K, using the new Cf-H_2O potentials for the cation-water interactions and the MCDHO model for the water-water interactions were carried out. Structures for analysis were taken from a statistical sampling of 2 Giga configurations. The MC simulation using the Cf-H_2O potential derived from the BP86 potential energy surface (BP86 simulation) leads to an average coordination number for the first coordination shell close to 8 (7.5), and the first maximum of the Cf-O RDF appears at 2.43 Å, whereas the MC simulation which uses the Cf-H_2O potential derived from the MP2 potential energy surface (MP2 simulation) gives a hydration number close to 9 (8.8) and the maximum for the Cf-O RDF appears at 2.53 Å. These general trends are in agreement with the QM study of An(III) aquaions recently reported by Dolg and col.[12a] The second coordination shell is formed by 16-17 (BP86 simulation) and 18-19 (MP2 simulation) water molecules centered at 4.65 and 4.69 Å, respectively. The absence of other experimental properties which could be compared with the predicted value derived from the statistical modelisation precludes the adoption of a convincing criterium to clearly select an intermolecular potential with respect to the other.

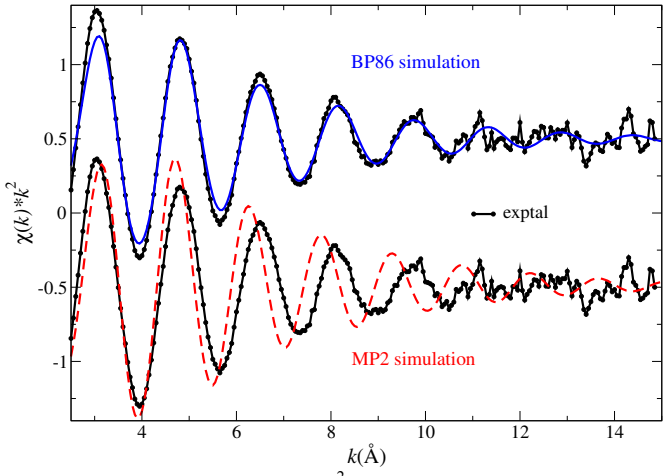

Figure 3. Comparison of the k^2-weighted Cf-L_{III} edge EXAFS spectrum of a 1mM Cf(III) aqueous solution in perchloric acid with the computed spectra obtained from the set of snapshots of the MC BP86 (blue line) or MP2 (red line) simulation.

The third step in this study is to combine the experimental and the theoretical results. The question to answer is which simulation provides a better agreement with the experimental results, and consequently which is the hydration number. The computation of XAS spectra from the structural information provided by computer simulations has proven a powerful tool for solving delicate structural problems such as the determination of the second shell.[15] 2000 configurations from each MC simulation have been selected to compute individually the Cf L_{III}-edge EXAFS spectra applying the FEFF code (version 8.4).[16] Different cutoff radii (R_{cut}= 3.5 - 5.5 Å) have been employed to examine the number of hydration shells which affect the EXAFS signal. This study has determined that the second hydration shell has a really marginal influence on the final computed spectrum. This is contrary to the cases of other lighter trivalent cations as Cr(III) [15b] or Ir(III),[15d] where the high stability of the first shell maintains a robust second hydration shell which indeed contributes to the backscattering signal. For the Cf(III) structure, as already reported for other lanthanoid[17] and actinoid[4d] cations, the water exchange and high fluxionality of the first shell preclude a stable enough second shell to contribute to the backscattering signal significantly. The k^2-weighted EXAFS spectra averaged on all structures taken from the BP86 and MP2 simulations (see Figure S2 in Supporting Information) are plotted in Figure 3, and compared with the experimental spectrum. The only parameter of the simulated spectra which was fitted with respect to the experimental one, was the value employed for E_o, what was chosen to best phase the computed signal with the experimental data. The agreement between simulated and experimental spectra is remarkable for the case of the BP86 simulation, where the intensity of the signal and the in-phase behaviour is maintained up to where the experimental spectrum is blurred by the high noise/signal ratio. For the case of the MP2 simulation, the computed spectrum shows an intensity less similar to the experimental one and a progressive out-phase behaviour due to the higher frequency of the computed EXAFS oscillations. Bearing in mind that the first computed spectrum is derived from the BP86 MC simulation which describes an average hydration number of eight around the Cf(III) cation, whereas the second computed spectrum comes from the MP2 MC simulation which describes an average hydration number of nine around the Cf(III) cation, we must conclude that Cf(III) aquaion is mainly octacoordinated and its average mean Cf-O distance is around 2.43Å.

The extremely close agreement between the BP86 simulated and experimental EXAFS spectra represents a strong support for the quantitative characterization of the hydration structure around Cf(III). Additional analysis can be done to get insight into the factors determining the ability of the methodology to reproduce the experimental EXAFS spectrum. The first point to be explored is the influence of the QM level employed and the second one is the role of the statistical sampling. We have computed four EXAFS spectra using only one structure of the Cf(III) aquaion, instead of averaging on a wide set of statistically-generated structures. We have employed the $[Cf(H_2O)_8]^{3+}$ and $[Cf(H_2O)_9]^{3+}$ optimized geometries at the MP2 and BP86 levels in both cases. (see Figure S2 in Supporting Information). Figure 4 plots the four spectra together with the experimental one. The intensity of all the simulated spectra is much higher than the experimental one, contrary to that observed in the computed spectra derived from the average of the statistical sampling (see Figure 3). This is a consequence of the lack of a DW factor applied to these model structures. However, the spectra computed from the MC simulations show how the fluctuations of the near Cf(III) environment supplied by the statistical average represents pretty well the structural distortions of the aquaions. In other words, the statistical average borne by the MP2 and BP86 simulations implicitly includes the DW factors, whereas the use of only one structure, even though it was the QM optimized is lacking of the disorder accounted by the DW factors. The second interesting conclusion derived from the analysis of Figure 4 with respect to Figure 3 is that the coordination number (solid line for CN=8 and dashed line for CN=9) is more determinant than the computational level (blue line for the BP86 optimized structures and red line for the MP2 ones). There is not a clear preference for a given QM model. A third remark is that even for the eight-fold coordination, a

phase-shift of the computed spectra is found, whereas this is not found in the statistically averaged BP86 EXAFS spectrum. This additional improvement in the BP86 statistically averaged spectrum indicates that beyond the intrinsic disorder included, responsible of the correct intensity of the signal, the average of single and multiple scattering contributions to the EXAFS spectrum subtly change the phase of the signal as a function of the *k* value. Therefore, this result leads us to conclude that the elucidation of the hydration number based on the consideration of different rigid aquaion models fails for highly dynamics aquaions.

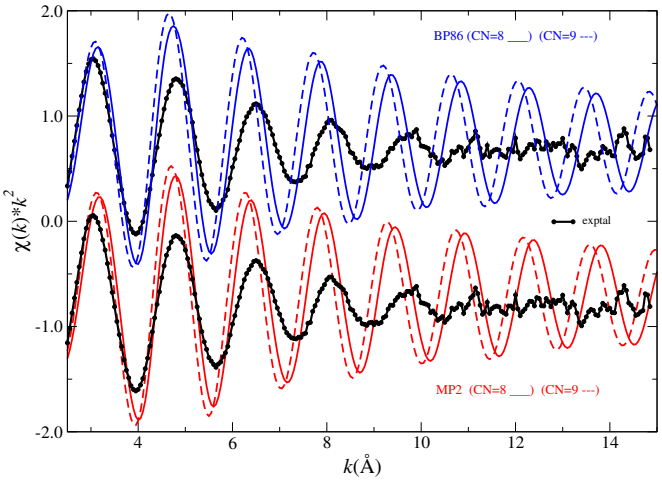

Figure 4. Comparison of the k^2-weighted Cf-L_{III} edge EXAFS spectrum of a 1mM Cf(III) aqueous solution in perchloric acid with the computed spectra obtained from the optimized MP2 (red lines) and BP86 (blue lines) structures corresponding to the $[Cf(H_2O)_8]^{3+}$ (solid lines) and $[Cf(H_2O)_9]^{3+}$ (dashed lines) aquaions.

Summarizing, the first Monte Carlo simulation on the trivalent cation of Californium, based on an exchangeable hydrated ion-water intermolecular potential, has been shown to represent an extended and improved methodology of the hydrated ion model.[13] Likewise, the Cf L_{III}-edge EXAFS spectrum of an acidic 1 mM $Cf(ClO_4)_3$ aqueous solution recorded under optimized experimental conditions, has greatly improved the signal/noise ratio of the only precedent recorded spectrum.[9] The comparison of the experimental EXAFS spectrum with the two computed ones, obtained from two different intermolecular potentials, which predict 8 (BP86) or 9 (MP2) water molecules in the first shell, leads to conclude that the lowest hydration number is preferred. Then, as far as Cf(III) is the heaviest actinoid aquaion for which there is experimental information, the actinide contraction is supported by the present study. (For U(III),$R_{U\text{-}O}$=2.56Å and CN=9±1;for Pu(III), $R_{Pu\text{-}O}$=2.51Å and CN=9±1; for Cm(III), $R_{U\text{-}O}$=2.45Å and CN=10±1).[3a] The role of the second hydration shell is important in defining the structure and dynamics of the Cf(III) aquaion, but its contribution to the EXAFS signal as backscatters is marginal.

Finally, this work gives an illustrative example of the benefits which can be achieved from the combination of the experimental XAS spectroscopies and computer simulations. The synergy to achieve an answer from the simultaneous analysis of the results, when each technique independently was not able to do it, has been clearly demonstrated in this work, as well as the importance of the structural statistical averages. We believe that this study traces a still non-well explored combined methodology which certainly may be extremely useful for many other complexes and limit chemical problems. A systematic theoretical and experimental examination of the other known actinoid cations on the same foot should be undertaken to confirm the findings here presented.

Experimental Section

Sample Preparation: A ten-year old solution of ^{249}Cf was the starting material. The initial cloudy solution was centrifuged and the supernatant percolated on a column filled with an anion exchanger (Bio-Rad AG-MP 1, 100-200 mesh). Then the eluted fractions were evaporated to dryness and taken up in dilute HCl. This solution was percolated through a column filled with a cation exchanger (Bio-Rad AG-MP 50, 100-200 mesh). The whole procedure was repeated twice. The purified fractions were gathered, evaporated to dryness and dissolved in $HClO_4$ 0.1M. The gamma spectrum of a fraction of the sample used for the EXAFS measurements exhibits the main γ-rays of ^{249}Cf: 387.95, 333.44 and 252.88 keV. The corresponding EXAFS sample (0.0022M) was loaded in a 200µL double layered Teflon/stainless steel cell, thus the masse of californium in the sample cell was 0.11mg.

EXAFS Data acquisition and processing : Californium L_{III}-edge XAS spectra were recorded at the European Synchrotron Radiation Facility (ESRF) (6 GeV at 200 mA), Rossendorf beam line (BM20). Measurements were carried out at room temperature, in 200 µL double layered Teflon/stainless stell cells. BM20 is equipped with a water cooled double crystal Si(111) monochromator. Higher harmonics were rejected by two collimating Pt coated mirrors. A 13-element Ge solid state detector was used for data collection in the fluorescence mode. Monochromator energy calibration was carried out at Mo K-edge (20000 eV). Data were processed using the Athena code[18]. Background removal was performed using a pre-edge linear function. Atomic absorption was simulated with a cubic spline function.

Data fitting : The extracted EXAFS signal was fitted in *R*-space without any additional filtering using the ARTEMIS code.[18] All adjustments were performed between 1 and 5 Å. Only two types of single-scattering paths were considered : Cf-O and Cf.....H paths. The $\Re$ factor and quality factor $\Delta\chi^2_\nu$ are both provided as an indication of the fit quality in *R* space while the average noise of the spectrum ε was estimated with back Fourier transformation in $k^2\chi(k)$ mode above 6 Å with the Cherokee code.[19] In all the fits, only one global amplitude factor and one energy threshold factor were considered for all the contributions. The Cf....H path length was linked to the Cf-O path length. It did not affect significantly the fit. Phases, amplitudes and electron mean free path were calculated with FEFF code based on two model structures obtained by quantum chemical calculations: the optimized structures of $[Cf(H_2O)_8]^{3+}$ (SA) and $[Cf(H_2O)_9]^{3+}$ (TTP).

*Cf-H_2O Intermolecular potentials and Monte Carlo Simulations.*The interactions of the metal ion with the water molecules are described by an exchangeable hydrated ion-water potential which is a modified model of the intermolecular potentials based on the hydrated ion concept.[13] The polarisable character of Cf(III) and water molecules is described by means of a shell-model. Details of this new development are given elsewhere.[14] The functional form adopted by this new potential is:

$$U_{inter} = \sum_{S=1}^{N}\left(\sum_{T=1}^{S-1}\left\{\sum_{i\in S}\sum_{j\in T}\left[U_{inter}(Z_i,Z_j)+U_{inter}(q_i,q_j)+U_{inter}(q_i,Z_j)+U_{inter}(q_j,Z_i)\right]\right\}+\sum_{i\in S}\frac{1}{2}k_i r_{ii}^2\right)$$

where

$$U_{inter}(X_i,X_j)=A\cdot e^{(-Br_{ij})}+C\cdot e^{(-Dr_{ij})}+\frac{X_iX_j}{r_{ij}}$$

is the functional form describing the intermolecular interaction between the nuclei Z_i and Z_j , $U_{inter}(Z_i ,Z_j)$, or density charges of the shell, q_i and q_j, $U_{inter}(q_i ,q_j)$; and

$$U_{inter}(q_i,Z_j)=\frac{q_iZ_j}{r_{ij}}\left[1-\left(\frac{r_{ij}}{\lambda_i}+1\right)\exp\left(-\frac{2r_{ij}}{\lambda_i}\right)\right]$$

is the functional form describing the interaction between the nucleus, Z_j, and the density charge, q_i.

The interaction energies to be fitted are obtained from ab initio calculations using the MP2 and DFT methods. The BP86 functional was used for the DFT calculations. A quasi-relativistic effective core potential (ECP87MWB type) specifically developed for the Cf(III) by Dolg and col.[12b] was employed together with their recommended basis sets for the valence orbitals, aug-cc-pvdz basis sets were used for the O and H atoms.
Simulations were carried out with the Monte Carlo Metropolis algorithm in the canonical ensemble (*NVT*) with periodic boundary conditions and Ewald summation to compute the electrostatic interactions. The side length of the cubic box was fitted to reproduce the density of water at 300K.

EXAFS spectrum computations. From each of the MC simulation, MP2 and BP86, a set of 2000 snapshots were taken for the simulation of the spectrum. As presented in previous works,[15a,b] the EXAFS function is obtained by averaging the individual $\chi_s(k)$ computed for each snapshot. Then the disorder arises from the non-symmetric arrangement of each snapshot and from summing over the representative number (N_s) of MC structural arrangements. This procedure differs from the classical formalism of the EXAFS equation[20] since the Debye-Waller factors associated to the different scattering paths are excluded from the expression employed, being replaced by the sum and average over N_s structures:

$$\chi(k)=\frac{1}{N_s}\sum_{s}^{N_s}\chi_s(k)=\frac{1}{N_s}\sum_{s}^{N_s}\sum_{j}^{paths}\frac{N_j S_o^2}{kR_{sj}^2}\left|f^{eff}(k,R)\right|\cdot\sin(2kR_{sj}+\varphi_j(k))e^{-2R_{sj}/\lambda}$$

where *s* goes over the structures obtained from the statistical sampling, and *j* goes over all the paths generated from each structure, restricted to a given cutoff ($R_{Cf\text{-}O}$= 3.5 or 5.5 Å). Typically, 25 or 50 paths are included when $R_{Cf\text{-}O}$ is 3.5 or 5.5 Å, respectively. XAS calculations were performed with the FEFF program (version 8.40)[16c]. The scattering potentials and the Fermi level are calculated self-consistently using the Hedin-Lundqvist functional. For the computation of the spectra derived from the BP86 and MP2 QM optimized structures, the same FEFF calculation level was applied. The constant shift applied to the Fermi level was, -5 eV for the BP86 simulation, whereas +1 eV was used for the MP2 simulation. One representative FEFF input file is given as supporting information.

Received: ((will be filled in by the editorial staff))
Published online on ((will be filled in by the editorial staff))

Keywords: Cf-water potential · EXAFS · MC simulation · Computed spectrum · Actinide contraction

[1] R. J. Silva, H. Nitsche, *Radiochim. Acta* **1995**, *70-71*, 377-396.
[2] M.. A. Denecke, *Coord. Chem. Rev.* **2006**, *250*, 730-754.
[3] a)S. Skanthakumar, M. R. Antonio, R. E. Wilson, L. Soderholm, *Inorg. Chem.* **2007**, *46*, 3485-3491; P.Lindqvist-Reis, C. Apostolidis, J. Rebizant, A. Morgenstern, R. Klenze, O. Walter, T. Fanghanel, R.G. Haire, *Angew.Chem. Int. Ed.* **2007**, *46*, 919-922.
[4] a)T. Yang, B. E. Bursten, *Inorg. Chem.* **2006**, *45*, 5291-5301; b) N.M.Edelstein, R. Klenze, T. Fanghanel, S. Hubert, *Coord. Chem. Rev.***2006**, *250*, 948-973; c) P. Lindqvist-Reis, C. Walther, R. Klenze, A. Eichhofer, T. Fanghanel, *J. Phys. Chem. B* **2006**, *110*, 5279- d) D. Hagberg, E. Bednarz, N. M. Edelstein, L. Gagliardi, *J. Am. Chem. Soc.* **2007**, *129*, 14136-14137.
[5] a)T. Tamaguchi, M. Nomura, H. Wakita, H. Ohtaki, *J. Chem. Phys.* **1988**, *89*, 5153-5159, b) G.T. Seaborg, *Radiochim. Acta* **1993**, *61*, 115-122.
[6] a) I. Persson, P. D'Angelo, S. de Panfilis, M. Sandström, L. Eriksson, *Chem. Eur. J.* **2008**, *14*, 3056-3066; b) P. D'Angelo, S. de Panfilis, A. Filipponi, I. Persson *Chem. Eur. J.* **2008**, *14*, 3045-3055
[7] a) F.H.David, B.Fourest, *New. J. Chem.* **1997**, *21*, 167-176; b) A. Bilewicz, *Radiochim. Acta* **2004**, *92*, 69-72.
[8] M. R. Antonio, C. W. Williams, L. Soderholm *Radiochim. Acta* **2002**, *90*, 851-856
[9] R. Revel, C. Den Auwer, C. Madic, F. David, B. Fourest, S. Hubert, J.-F. Le Du, L. R. Morss, *Inorg. Chem.* **1999**, *38*, 4139-4141.
[10] H. Saint-Martin, J. Hernández-Cobos, M. I. Bernal-Uruchurtu, I. Ortega-Blake, J. C. Berendsen, *J. Chem. Phys.* **2000**, *113*, 10899-10912.
[11] K. Schmeide, T. Reich, S. Sachs, G. Bernhard, *Inorg.Chim.Acta* **2006**, *359*, 237-242.
[12] a) J. Wiebke, A. Morit X. Cao, M. Dolg, *Phys.Chem Chem. Phys.* **2007**, *9*, 459-465; b) A. Moritz, X. Y. Cao, M. Dolg, *Theor.Chem Acc.* **2007**, *117*, 473-481.
[13] a) R. R. Pappalardo, E. Sánchez Marcos, *J. Phys. Chem.* **1993**, *97*, 4500-4504; b) J. M. Martínez, R. R. Pappalardo, E. Sánchez Marcos, *J. Am. Chem. Soc.* **1999**, *121,* 3175-3184; c) J. M. Martínez, F. Torrico, R. R. Pappalardo, E. Sánchez Marcos, *J. Phys. Chem. B* **2004**, *108*, 15851-15855.
[14] J. Hernández-Cobos, E. Galbis, R. R. Pappalardo and E. Sánchez Marcos, in preparation.
[15] a) P. J. Merkling, A. Muñoz-Páez, J. M. Martínez, R. R. Pappalardo, E. Sánchez Marcos, *Phys. Rev. B* **2001**, *64*, 012201-4; b) P. J. Merkling, A. Muñoz-Páez, E. Sánchez Marcos, *J. Am. Chem. Soc.* **2002**, *124*, 10911-10920, c) P. D'Angelo, O. M. Roscioni, G. Chillemi, S. Della Longa, M. Benfatto, *J. Am. Chem. Soc.* **2006**, *128*, 1853-1858; d)F. Carrera, F. Torrico, D.T.Richens, A. Muñoz-Páez, J.M.Martínez, R. R. Pappalardo, E. Sánchez Marcos J. Phys. Chem. B **2007**, *111,* 8223-8233.
[16] a)A.L.Ankudinov, B.Ravel, J.J.Rehr, S.D. Conradson, *Phys. Rev. B* **1998**, *58*, 7565-7576; b) J.J. Rehr, R.C. Albers, *Rev. Mod.Phys.* **2000**,*72,* 621- 654; c)A.L.Ankudinov, A.I.Nesvizhskii, J.J:Rehr, *Phys. Rev. B* **2003**, *67,* 115120.
[17] a)L. Helm, A. E. Merbach, *Chem. Rev.* **2005**, *105*, 1923-1960; b)M. Duvail, P. Vitorge, R. Spezia, *J.- Chem. Phys.* **2009**, *130*, 104501 ;c) A. Villa, B. Hess, H. Saint-Martin, *J. Phys. Chem. B* **2009**, *113*, 7270-7281.
[18] B. Ravel, M. Newville, *J. Synchrotron Rad.* **2005**, *12*, 537-541.
[19] A. Michalowicz, EXAFS code available at http://icmpe.cnrs.fr
[20] D.E. Sayers, E.A.Stern, F.W.Lytle, *Phys. Rev. Lett.* **1971**, *27*, 1204-1207.

Entry for the Table of Contents

Proving Actinide Contraction

Elsa Galbis Fuster, Jorge Hernández-Cobos, Christophe den Auwer*, Claire Le Naour, Dominique Guillaumont, Eric Simoni, Rafael R. Pappalardo, Enrique Sánchez Marcos*___ **Page – Page**

Solving the hydration structure of the heaviest actinoid aquaion known: the Californium(III) case

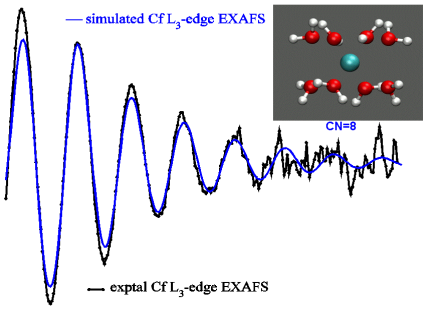

X-ray Absorption Spectroscopy and Monte Carlo simulations of Cf(III) in aqueous solutions have been combined to determine the distance and coordination number of the Cf(III) aquaion, the heaviest cation measured and simulated. The results obtained supports that in the actinide series a contraction takes place as in the lanthanide series.

SUPPORTING INFORMATION

Table S1. Formation energies (kcal/mol) for different Cf(III) aquaions predicted by the quantum-mechanical BP86 and MP2 methods and the new Cf-H_2O interaction potentials plus MCDHO water potential.(Aquaion geometries correspond to the quantum-mechanical optimized ones).

Aquaion	ΔE_{form}			
	QM-BP86	BP86 Potential	QM-MP2	MP2 Potential
$[Cf(H_2O)_8]^{3+}$	-486.0	-485.0	-502.4	-503.1
$[Cf(H_2O)_9]^{3+}$	-505.4	-502.2	-528.1	-525.7
$[Cf(H_2O)_8]^{3+}\cdot(H_2O)_{16}$	-801.8	-810.6	-850.2	-827.2
$[Cf(H_2O)_9]^{3+}\cdot(H_2O)_{18}$	-813.7	-835.6	-886.1	-851.8

Figure S1. Comparison of the geometries predicted by the quantum-mechanical level (blue) and the intermolecular potentials (red)

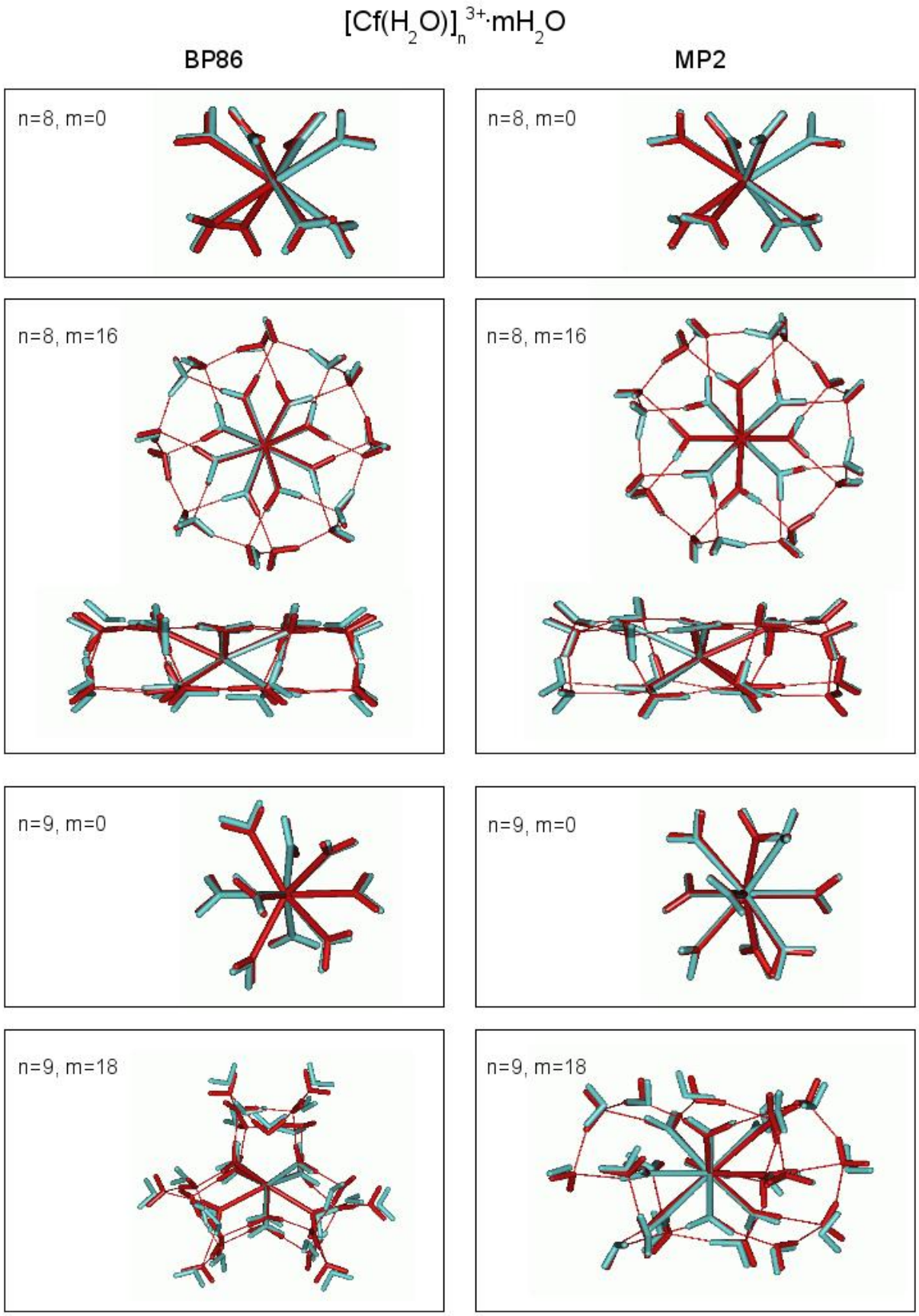

Figure S2. Scheme of the two different methods employed to compute the EXAFS spectrum from the snapshots of the MC simulation or the quantum mechanical optimized structures.

Snapshots of MC simulations

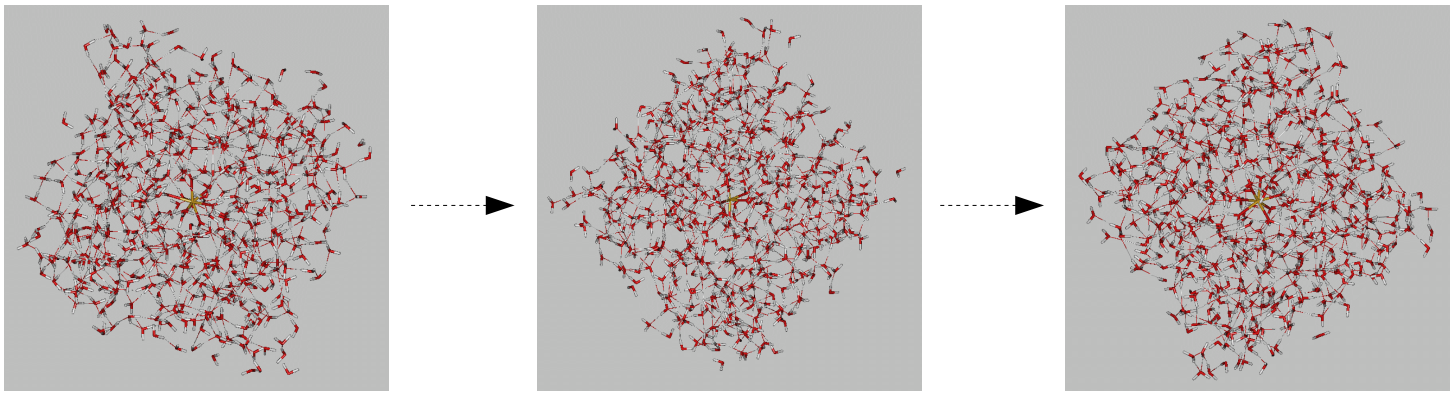

Computed EXAFS spectra

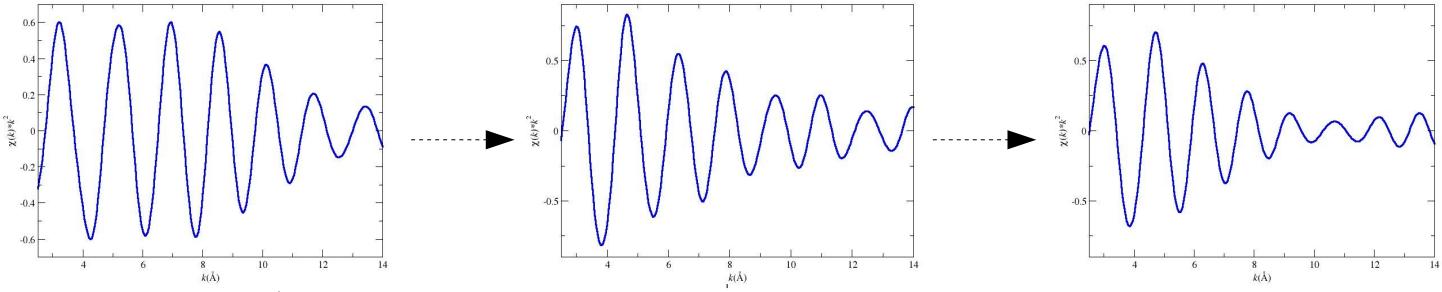

Average computed EXAFS spectra

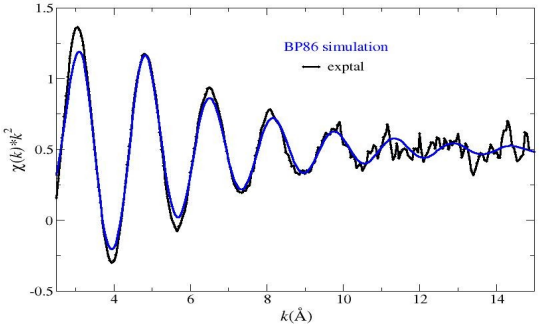

QM optimized structures

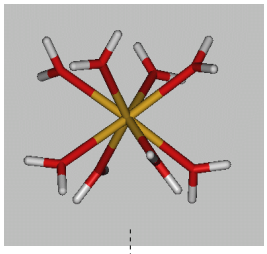

$[Cf(H_2O)_8]^{3+}$

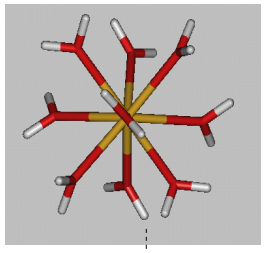

$[Cf(H_2O)_9]^{3+}$

Computed EXAFS spectra

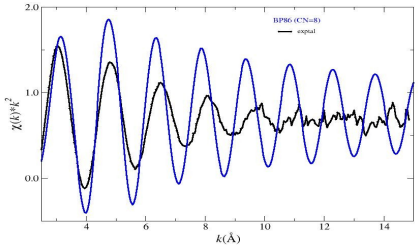

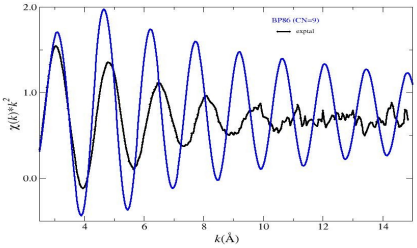

Input FEFF File for the simulation of an EXAFS spectrum from a MC simulation snapshot.

```
TITLE Cf structure snapshot serie BP86  R_cut=3.5 A
TITLE Part 1

HOLE 4   1.0     Cf  L-III edge  (    keV), s0^2=1.0

 POTENTIALS
*   ipot   z  label   l
       0    98  Cf     3   3
       1    8    O     3   3
       2    1    H     2   2

*         mphase,  mpath,  mfeff,  mchi
CONTROL     1       0       0       0       0      0
*CONTROL    0       1       1       1       1      1
 PRINT      0       0       0       3

TDLDA  1
SCF       4.0   0

EXCHANGE  0   -5.0   0.
CRITERIA 4.0 2.5
RPATH 6.0
NLEG 4

S02 1.00
ATOMS
   0.0000000    0.0000000    0.0000000  0  Cf    0.0000000
  -2.3223400   -0.3302100    0.0492400  1  O     2.3462153
  -3.1309500   -0.2257400    0.7162700  2  H     3.2197592
  -2.7968400   -0.6640100   -0.7768500  2  H     2.9777037
  -0.2550800   -0.9478800   -2.1422600  1  O     2.3564423
  -0.0826100   -1.9242100   -2.3877000  2  H     3.0676571
  -0.4171400   -0.4563700   -3.0428500  2  H     3.1050307
   0.3346700   -0.0634500    2.3325000  1  O     2.3572412
  -0.0895000   -0.7549000    2.9250400  2  H     3.0222083
   0.5877600    0.7381400    2.8843800  2  H     3.0347917
   1.9754700   -1.3182500    0.0210900  1  O     2.3750178
   2.5544900   -1.6879100   -0.6862500  2  H     3.1377378
   2.5629300   -1.4647300    0.7715700  2  H     3.0511251
   1.8499500    1.4163300   -0.5915300  1  O     2.4037915
   2.3292900    2.2458000   -0.2245300  2  H     3.2433969
   2.5120100    1.1898300   -1.3076000  2  H     3.0717597
  -0.6244900    2.1256700    1.0730200  1  O     2.4616727
  -0.2756700    3.0819200    0.8753900  2  H     3.2156698
  -1.5220300    2.3216900    1.4396200  2  H     3.1271913
  -0.7930300   -2.4142700    0.8952000  1  O     2.6942493
  -1.6215700   -2.6360100    1.4281600  2  H     3.4084716
  -0.2853100   -3.1960300    0.9691900  2  H     3.3519157
  -0.8726600    2.1459700   -2.2100600  1  O     3.2017320
  -1.2278000    1.9714800   -3.0793600  2  H     3.8570305
  -0.0555400    2.6051800   -2.4950400  2  H     3.6076685
END
```

```
TITLE Cf structure snapshot serie BP86 R_cut=3.5 A
TITLE Part 2

HOLE 4   1.0     Cf L-III edge  (    keV), s0^2=1.0

 POTENTIALS
*   ipot   z  label  l
       0    98  Cf    3   3
       1    8    O     3   3
*       2    1    H     2   2

*         mphase,  mpath,  mfeff,  mchi
*CONTROL     1       0       0       0       0      0
CONTROL    0       1       1       1       1      1
 PRINT      0       0       0       3

TDLDA  1
SCF   4.0  0

EXCHANGE  0   -5.0  0.
CRITERIA 4.0 2.5
RPATH 6.0
NLEG 4
S02 1.00
ATOMS
   0.0000000    0.0000000    0.0000000  0  Cf    0.0000000
  -2.3223400   -0.3302100    0.0492400  1  O    2.3462153
  -0.2550800   -0.9478800   -2.1422600  1  O    2.3564423
   0.3346700   -0.0634500    2.3325000  1  O    2.3572412
   1.9754700   -1.3182500    0.0210900  1  O    2.3750178
   1.8499500    1.4163300   -0.5915300  1  O    2.4037915
  -0.6244900    2.1256700    1.0730200  1  O    2.4616727
  -0.7930300   -2.4142700    0.8952000  1  O    2.6942493
  -0.8726600    2.1459700   -2.2100600  1  O    3.2017320
END
```